Mathematics of thermoacoustic and photoacoustic tomography

Peter Kuchment[*]and Leonid Kunyansky[†]

Abstract

The paper presents a survey of mathematical problems, techniques, and challenges arising in the Thermoacoustic and Photoacoustic Tomography.

1   Introduction

Medical tomography has had a huge impact on medical diagnostics. Numerous methods of tomographic medical imaging have been developed and are being developed (e.g., the "standard" X-ray, single-photon emission, positron emission, ultrasound, magnetic resonance, electrical impedance, optical) [44, 48, 64, 65, 66]. The designers of these modalities strive to increase the image resolution and contrast, and at the same time to reduce the costs and negative health effects of these techniques. However, these goals are usually rather contradictory. For instance, some cheap and safe methods with good contrast (like optical or electrical impedance tomography) suffer from low resolution, while some high resolution methods (such as ultrasound imaging) often do not provide good contrast. Recently researchers have been developing novel methods that combine different physical types of signals, in hope to alleviate the deficiencies of each of the types, while taking advantage of their strengths. The most succesfull example of such a combination is the **Thermoacoustic Tomography (TAT)** (also abbreviated as TCT) [50].

[*]Mathematics Department, Texas A& M Univeristy, College Station, TX 77845. kuchment@math.tamu.edu

[†]Mathematics Department, Univeristy of Arizona, Tucson, AZ. leonk@math.arizona.edu

After a substantial effort, major breakthroughs have been achieved in the last couple of years in the mathematical modeling of TAT. The aim of this article is to survey this recent progress and to describe the relevant models, mathematical problems, and reconstruction procedures arising in TAT and in its sibling, photoacoustic tomography (PAT).

It is useful to notice that mathematical problems of the same type as in TAT, arise also in sonar and radar research (e.g., [62, 69]).

The engineering literature on TAT/PAT is rather vast and no attempt has been made in this text to create a comprehensive bibliography of the topic. The authors, however, have tried to present a concise review of the existing (not very extensive) literature on mathematics of this imaging method, although some publications might have been inadvertently omitted.

2   Thermoacoustic and photoacoustic tomography

In TAT, a very short radiofrequency (RF) pulse is sent through a biological object (e.g., woman's breast in mammography).
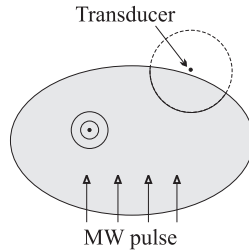

Figure 1: The TAT procedure.

The set-up is such that the whole object is more or less uniformly irradiated. Some part of RF energy is absorbed throughout the object, and this causes thermoelastic expansion of the tissue and emergence and propagation of a pressure wave $p(x,t)$ (an ultrasound signal) that can be measured by transducers placed around the object. Ultrasound imaging by itself suffers from low contrast. It is known, however, (e.g., [50, 96]) that cancerous cells absorb several times more energy in the RF range than the healthy ones. Thus, function $f(x)$ describing spatial distribution of the absorption of RF

2

energy, and therefore, the intensity of the source of the acoustic wave will have a very good contrast. Thus, if one could reconstruct $f(x)$, one would have an efficient tool for early detection of cancer. The smallness of the ultrasound contrast is in fact a good thing here, allowing one to assume in the first approximation that the sound speed is constant[1]. Now one can attempt to recover the function $f(x)$ (the image) from the measured data $p(x, t)$.

The photoacoustic tomography (PAT) differs from TAT only in the way the thermoacoustic signal is triggered. In PAT, in contrast to TAT, a laser pulse is used rather than an RF one to initiate the signal [95], while the rest of the procedure stays the same. From the mathematical point of view, there is no difference between TAT and PAT. Hence, in what follows, we will be just mentioning TAT.

In the next section we present a mathematical description of the relation between $f(x)$ and $p(x, t)$.

3 Mathematical model of TAT: wave equation and the spherical mean Radon transform

We assume, as it has already been mentioned before, that the visualized object is nearly homogeneous with respect to ultrasound and that the units are chosen in such a way as to make the speed of ultrasound equal to 1. Then, modulo some constant coefficients that we will assume to be equal to 1, the pressure wave $p(x, t)$ satisfies the following problem for the standard wave equation [21, 94, 96]:

$$\begin{cases} p_{tt} = \Delta_x p, t \geq 0, x \in \mathbb{R}^3 \\ p(x, 0) = f(x), \\ p_t(x, 0) = 0 \end{cases} \tag{1}$$

The goal is to find, using the data measured by transducers, the initial value $f(x)$ at $t = 0$ of the solution $p(x, t)$.

---

[1]This approximation is not always appropriate, but it is the best studied case at the moment. One can look at [46, 53] for some initial studies of the case of non-constant sound speed.

In order to formalize what data is in fact measured, one needs to specify what kind of transducers is used, as well as the geometry of the measurement. By the geometry of the measurement we mean the distribution of locations of transducers used to collect the data.

We briefly describe here the commonly considered measurement procedures. It is too early to judge which one of them will become most successful, but the one using point transducers has been more thoroughly studied mathematically and experimentally, and thus will occupy most of the space in this article. In this (most commonly used so far) case, the transducers are assumed to be point-like, i.e. of sufficiently small dimension. A transducer at time t measures the average pressure over its surface at this time, which for the small size of the transducer can be assumed to be just the value of $p(y, t)$ at the location y of the transducer. Dimension count shows immediately that in order to have enough data for reconstruction of the function $f(x)$, one needs to collect data from the transducers' locations y running over a surface S in $\mathbb{R}^3$. Thus, the data at the experimentator's disposal is the function $g(y, t)$ that coincides with the restriction of $p(x, t)$ to the set of points $y \in S$.

There are two ways to describe the relation between the data $g(y, t), (y, t) \in S \times \mathbb{R}^+$ and the image $f(x), x \in \mathbb{R}^3$ to be recovered. The first one deals with the wave equation. Taking into account that the measurements produce the values $g(y, t)$ of the pressure $p(x, t)$ of (1) on $S \times \mathbb{R}^+$, the set of equations (1) extends to become

$$\begin{cases} p_{tt} = \Delta_x p, t \geq 0, x \in \mathbb{R}^3 \\ p(x, 0) = f(x), \\ p_t(x, 0) = 0 \\ p(y, t) = g(y, t), y \in S \times \mathbb{R}^+ \end{cases} \quad (2)$$

The problem now becomes finding the initial value $f(x)$ in (2) from the knowledge of the lateral data $g(x, t)$ (see Figure 3). A person familiar with PDEs might suspect first that there is something wrong with this problem, since we seem to have insufficient data when recovering the solution of the wave equation in a cylinder from the lateral values alone. This, however, is an illusion, since in fact there is a significant additional restriction: the solution holds in the whole space, not just inside the cylinder $S \times \mathbb{R}^+$. We will see soon that in most cases, the data is sufficient for recovery of $f(x)$.

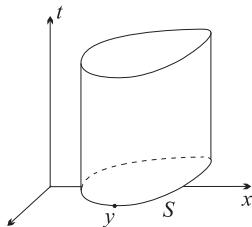We now introduce an alternative formulation of the problem. The known

4

Figure 2: An illustration to (2).

Poisson-Kirchhoff formula [19, Ch. VI, Section 13.2, Formula (15)] for the solution of (1) gives

$$p(x,t) = c\frac{\partial}{\partial t}\left(t(Rf)(x,t)\right), \tag{3}$$

where

$$(Rf)(x,r) = \int_{|y|=1} f(x+ry)dA(y) \tag{4}$$

is the *spherical mean operator* applied to the function $f(x)$, and dA is the normalized area element on the unit sphere in $\mathbb{R}^3$.

Thus, knowledge of the function $g(x,t)$ for $x \in S$ and all $t \geq 0$ essentially means knowledge of the spherical mean $Rf(x,t)$ at all points $(x,t) \in S \times \mathbb{R}^+$. One thus is lead to studying the spherical mean operator $R : f \to Rf$ and in particular its restriction R_S to the points $x \in S$ only (these are the points where we place transducers):

$$R_S f(x,t) = \int_{|y|=1} f(x+ty)dA(y), x \in S, t \geq 0. \tag{5}$$

This is why, in many works on thermoacoustic tomography, the spherical mean operator has been the model of choice. Albeit the (unrestricted) spherical mean operator has been studied rather intensively and for a long time (e.g., [14, 19, 47]), its version R_S with the centers restricted to a subset S appears to have been considered since early 1990s only and offers quite a few new and often hard questions.

In what follows, we will alternate between these two (PDE and integral geometry) interpretations of the TAT model, since each of them has its own advantages.

5

3.1 Main mathematical problems of TAT

We now formulate the typical list of problems one would like to address in order to implement the TAT reconstruction. We will state them in terms of the spherical mean operator, albeit they can be easily rephrased in terms of the wave equation.

1. For which sets $S \in \mathbb{R}^3$ is the operator R_S injective on an appropriate class of functions, say on continuous with compact supports? In other words, for which sets S the data collected by transducers placed along S is sufficient for unique reconstruction of f?

2. If R_S is injective, what are inversion formulas and algorithms?

3. How stable is the inversion?

4. What happens if the data is "incomplete"?

5. What is the range of the operator R_S in appropriate function spaces? This question might seem to be unusual for people coming from PDEs, but in integral geometry and tomography importance of knowing the range of Radon type transforms is well known (e.g., [22, 28, 29, 30, 42, 43, 44, 65, 66, 75]).

4 Uniqueness of reconstruction

Many of the problems of interest to TAT can be formulated in any dimension d, which we will do whenever we can.

Let $S \subset \mathbb{R}^d$ be the set of locations of transducers and f be a compactly supported function of an appropriate class. As it is shown in [5], we can assume it to be infinitely smooth without reducing the generality. Does the equality $R_S f = 0$ (i.e., absence of the signal on the transducers) imply that $f = 0$? If the answer is a "yes," we call S - a **uniqueness set**, otherwise a **non-uniqueness set**. In other words, in terms of TAT, the uniqueness sets are those that distributing transducers along them provides enough data for unique reconstruction of the function $f(x)$.

In terms of the wave equation, uniqueness sets are the sets of complete observability, i.e. such that observing the motion on this set only, one gets enough information to reconstruct the whole oscillation.

We would like to discuss in this section the problem of describing all non-uniqueness sets (since, as we will see, most are the uniqueness ones). The following simple statement is very important and not immediately obvious.

Lemma 1. *[5, 60, 61, 101] Any non-uniqueness set S is a set of zeros of a (non-trivial) harmonic polynomial. In particular, any non-uniqueness set is algebraic and any uniqueness set for harmonic polynomials is also a uniqueness set for the spherical mean Radon transform.*

The proof of this lemma is very simple. It works under the assumption of exponential decay of the function $f(x)$, not necessarily of compactness of its support. It also introduces some polynomials that play significant role in the whole analysis of R_S.

Let $k \geq 0$ be an integer. Consider the convolution

$$Q_k(x) = |x|^{2k} * f(x) = \int |x - y|^{2k} f(y) dy. \tag{6}$$

This is clearly a polynomial of degree at most $2k$. Rewriting the integral in polar cooordinates centered at x and using radiality of $|x - y|$, one sees that the value $Q_k(x)$ is determined if we know the values $Rf(x,t)$ of the spherical mean of f centered at x:

$$Q_k(x) = c_d \int\limits_0^\infty t^{2k+d-1} Rf(x,t) dt.$$

In particular, If $R_S f \equiv 0$, then each polynomial Q_k vanishes on S.

Another observation that is easy to justify is that if the function f is exponentially decaying (e.g., is compactly supported), and if all polynomials Q_k vanish identically, the function itself must be equal to zero. (This is not true anymore if f is just fast decaying in the sense of the Schwartz space.)

Thus, we conclude that if f is not identically equal to zero, then there is at least one non-zero polynomial Q_k. Since, as we discussed, equality $R_S f = 0$ implies that $Q_k|_S = 0$, we conclude that S must be algfebraic.

Now notice the following simple to verify equality (with a non-zero constant c_k):

$$\Delta Q_k = c_k Q_{k-1}, \tag{7}$$

where Δ is the Laplace operator. This implies that the lowest k non-zero polynomial Q_k is harmonic. Since $Q_k|_S = 0$, this proves the lemma.

7

Consider now the case when S is a closed hypersurface (i.e., the boundary of a bounded domain). Since, as it is well known, there is no non-zero harmonic function in the domain that would vanish at the boundary (the spectrum of the Dirichlet Laplace operator is strictly positive), we conclude that such S is a uniqueness set for harmonic polynomials. Thus, we get

Corollary 2. *[5, 51] Any closed hypersurface is uniqueness set for the spherical mean Radon transform.*

An older alternative proof [51] of this corollary provides an additional insight into the problem, which happens to be useful in many circumstances. We thus sketch it here. Let us assume for simplicity that the dimension $d \geq 3$ is odd (even dimensions require a little bit more work). Suppose that the closed surface S remains stationary (nodal) for the oscillation described by (1). Since the oscillation is unconstrained and the initial perturbation is compactly supported, after a finite time, the interior of S will become stationary. On the other hand, we can think that S is fixed (since it is not moving anyway). Then, the energy inside S must stay constant. This is the contradiction that proves the statement of Corollary 2.

This corollary resolves the uniqueness problems for most practically used geometries. It fails, however, if f does not decay sufficiently fast (see [3], where it is shown in which $L^p(\mathbb{R}^d)$ classes of functions $f(x)$ closed surfaces remain uniqueness sets).

It also provides uniqueness for some "limited data" problems. For instance, if S is an open (even tiny) piece of an analytic closed surface Σ, it suffices. Indeed, if it did not, then it would be a part of an algebraic non-uniqueness surface. Uniqueness of analytic continuation would show then that the whole Σ is a non-uniqueness set, which we know to be incorrect. This result, however, does not say that it would be practical to reconstruct using observations from a tiny S. We will see later that this would not lead to a satisfactory reconstructions, due to instabilities.

Although, for all practical purposes the uniqueness of reconstruction problem is essentially resolved by the Corollary 2, the complete understanding of uniqueness problem has not been achieved yet. Thus, we include below some known theoretical results and open problems.

4.1 Non-uniqueness sets in $\mathbb{R}^2$.

In this subsestion, we follow the results and exposition of [5, 60, 61] in discussing uniqueness sets in $2D$. What are simple examples of non-uniqueness sets? It is clear that any line S (or a hyperplane in higher dimensions) is a non-uniqueness set. Indeed, any function f that is odd with respect to S will clearly produce no signal: $R_S f = 0$. Analogously, consider a *Coxeter system* Σ_N of N lines passing through a point and forming equal angles (see Fig. 3).
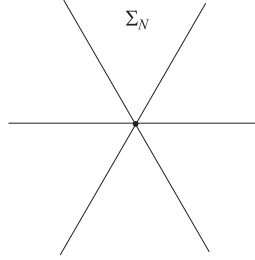

Σ_N

Figure 3: Coxeter cross Σ_N.

Choosing the intersection point as the pole and expanding functions into Fourier series with respect to the polar angle, it is easy to discover existence of an infinite dimensional space of functions that are odd with respect to each of the N lines. Thus, such a cross Σ_N is also a non-uniqueness set. Less obviously, one can use the infinite dimensional freedom just mentioned to add any finite set Φ of points still preserving non-uniqueness. The following major and very non-trivial result was conjectured in [60, 61] and proven in [5].

Theorem 3. *[5] A set $S \subset \mathbb{R}^2$ is a non-uniqueness set for the spherical mean transform in the space of compactly supported functions, if and only if*

$$S \subset \omega \Sigma_N \cup \Phi,$$

where Σ_N is a Coxeter system of lines, ω is a rigid motion of the plane, and Φ is a finite set.

A sketch of the proof. Suppose that f is compactly supported, not identically zero, and such that $R_S f = 0$. Our previous considerations show that one can assume that S is an algebraic curve (not a straight line) that is

9

contained in the set of zeros of a non-trivial harmonic polynomial. Now one touches the boundary of the support of f from outside by a circle centered on S. Then microlocal analysis of the operator R_S (which happens to be an analytic Fourier Integral Operator, FIO [15, 32, 33, 34, 35, 84]) shows that, due to the equality $R_S f = 0$, at the tangency point the vector co-normal to the sphere should not belong to the analytic wave front of f (microlocal regularity of solutions of $R_S f = 0$). This, for instance, can be extracted from the results of [93]. On the other hand, a theorem by Hörmander and Kashiwara [45, Theorem 8.5.6] (a microlocal version of uniqueness of analytic continuation) shows that this vector must be in the analytic wave front set, since $f = 0$ on one side of the sphere. This way, one gets a contradiction. Unfortunately, the life is not so easy, and the proof sketched above does not go through smoothly, due to possible cancellation of wavefronts at different tangency points. Then one has to involve the geometry of zeros of harmonic polynomials [27] to exclude the possibility of such a cancellation.

Thus, the proof uses microlocal analysis and geometry of zeros of harmonic polynomials. Both these tools have their limitations. For instance, the microlocal approach (at least, in the form it is usedn in [5]) does not allow considerations of non-compactly supported functions. Thus, the validity of the Theorem for arbitrarily fast decaying, but not compactly supported, functions is still not established, albeit it most certainly holds. On the other hand, the geometric part does not work that well in dimensions higher than two. Development of new approaches is apparently needed in order to overcome these hurdles. A much simpler PDE approach has emerged recently in [26] (see also [10] and the next Section), albeit its achievements in describing uniqueness sets have been limited so far.

4.2   Higher dimensions

Here we present the conjecture of how the result should look like in higher dimensions.

Conjecture 4. *[5]A set $S \subset \mathbb{R}^d$ is a non-uniqueness set if and only if $S \subset \omega \Sigma \cup \Phi$, where Σ is the surface of zeros of a homogeneous harmonic polynomial, ω is a rigid motion of $\mathbb{R}^d$, and Φ is an algebraic surface of codimension at least 2.*

The progress towards proving this conjecture has been slow, albeit some partial cases have been treated ([1]-[10]). E.g., in some cases one can prove
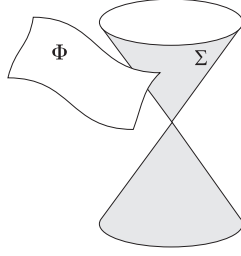
Figure 4: A picture of a d-dimensional non-uniqueness set.

that S is a ruled surface (i.e., consists of lines), so only proving that they pass through the same point remains a challenge. It is also known that the sets $\omega\Sigma$ and Φ of the type described in the conjecture, are non-uniqueness sets [2, 5].

4.3   Relations to other areas of analysis

The problem of injectivity of R_S has relations to a wide variety of areas of analysis (see [1, 5] for many examples). In particular, the following interpretation is important:

Theorem 5. *[5, 51] The following statements are equivalent:*

1. *$S \subset \mathbb{R}^d$ is a non-uniqueness set for the spherical mean operator.*

2. *S is a nodal set for the wave equation, i.e. there exists a non-zero compactly supported f such that the solution of the wave propagation problem*
$$\begin{cases} \frac{\partial^2 u}{\partial t^2} = \Delta u, \\ u(x,0) = 0, \\ u_t(x,0) = f(x) \end{cases}$$
   vanishes on S for any moment of time.

3. *S is a nodal set for the heat equation, i.e. there exists a non-zero*

11

compactly supported f such that the solution of the problem

$$\begin{cases} \frac{\partial u}{\partial t} = \Delta u, \\ u(x,0) = f(x) \end{cases}$$

vanishes on S for any moment of time.

The interpretation in terms of the wave equation provides important PDE tools and insights, which have lead to a recent progress [26, 10] (albeit it has not lead yet to a complete alternative proof of Theorem 3). The rough idea is that if S is a nodal set, then it might be considered as the fixed boundary. In this case, the signals must go around S. However, in fact, there is no obstacle, so signals can propagate along straight lines. Thus, in order to avoid discrepancies in arrival times, S must be very special. One can find details in [26] and in [10].

5   Reconstruction: formulas and examples

5.1   Inversion formulas

Placing transducers on a plane surface is, perhaps, the simplest acquisition geometry. Thus, the problem of recovering functions from integrals over spheres centered on a (hyper)plane S has attracted a lot of attention over the years. Although, as it has been mentioned before, there is no uniqueness in this case (functions odd with respect to S are annihilated), even functions can be recovered. Functions supported on one side of the plane can be reconstructed as well, by means of their even extension. Many explicit inversion formulas and procedures have been obtained for this situation [13, 20, 23, 29, 31, 66, 68, 74, 75, 89, 91]. We will not provide any details here, since this acquisition geometry does not seem to be very useful for TAT. In particular, this is due to "invisibility" of some parts of the interfaces, see Section 6, which arises from truncating the plane. The same problem is encountered with some other unbounded acquisition surfaces, such as a surface of an "infinitely" long cylinder.

Thus, it is more practical to place transducers along a closed surface surrounding the object. The simplest surface of this type is a sphere.

The first inversion procedures for the case of spherical acquisition were described in [70] in $2D$ and in [71] in $3D$. These solutions were obtained by

harmonic decompositon of the measured data and of the sought function, and then by equating coefficients of the corresponding Fourier series. Interestingly, the two series solutions are not quite analogous. While computing the coefficients of the angular Fourier series in [70] one has to divide the Hankel transform of the data by the Bessel functions that have infinitely many zeros. The $3D$ solution in [71], on the other hand, is free from this shortcoming. In fact, the techniques of [71] can also be adopted for $2D$.

The most popular way of inverting Radon transform in tomography applications is by using filtered backprojection type formulas. Such reconstructions are obtained by linear filtration of projections (either in Fourier domain, or by a convolution with a certain kernel) followed (or preceeded) by a backprojection. In the case of the set of spheres centered on a closed surface (e.g., sphere) S, one expects such a formula to involve a filtration with respect to the radial variable and some integration over the set of spheres passing through the point of interest. For quite a while, no such type formula had been discovered. This did not prevent practitioners from reconstructions, since good approximate inversion formulas (parametrices) could be developed, followed by an iterative improvement of the reconstruction, see e.g. reconstruction procedures in [82, 83, 95, 96, 98, 99, 100].

The first set of exact inversion formulas of the filtered backprojection type was discovered in [26]. These formulas were obtained only in odd dimensions. Several different variations of such formulas (different in terms of the sequence of filtration and backprojection steps) were developed.

Let us assume that B is the unit ball and $S = \partial B$ is the unit sphere in $\mathbb{R}^3$. We will reconstruct a function $f(x)$ supported inside S from the known values of its spherical integrals $g(z, r)$ with the centers on S:

$$g(z,r) = \int_{\mathbb{S}^{n-1}} f(z + rs) r^{n-1} ds = \omega_n r^{n-1} R_S f(z,r), \qquad z \in S. \qquad (8)$$

Then various versions of the $3D$ inversions formulas that reconstruct a function $f(x)$ supported inside S from its the spherical mean data $R_S f$, are

$$f(y) = -\frac{1}{8\pi^2 R} \Delta_y \int_{\partial B} g(z, |z - y|) dA(z),$$

$$f(y) = -\frac{1}{8\pi^2 R} \int_{\partial B} \left(\frac{1}{t} \frac{d^2}{dt^2} g(z,t) \right) \Bigg|_{t=|z-y|} dA(z). \qquad (9)$$

13

Recently, analogous formulas were obtained for even dimensions in [24]. Denoting by g, as before the spherical integrals (rather than averages) of f, the formulas in $2D$ look as follows:

$$f(y) = \frac{1}{2\pi R}\Delta \int_{\partial B} \int_0^{2R} g(z,t)\log(t^2 - |y-z|^2)\, dt\, dl(z),\qquad (10)$$

or

$$f(y) = \frac{1}{2\pi R}\int_{\partial B} \int_0^{2R} \frac{\partial}{\partial t}\left(t\frac{\partial}{\partial t}\frac{g(z,t)}{t}\right)\log(t^2 - |y-z|^2)\, dt\, dl(z),\qquad (11)$$

A different set of explicit inversion formulas that work in arbitrary dimensions was presented in [58].

In 2-D the formula takes form

$$f(y) = \frac{1}{8\pi}\mathrm{div}\int_S \mathbf{n}(z)h(z,|y-z|)dl(z),\qquad (12)$$

where

$$h(z,t) = \int_{\mathbb{R}^+}\left[N_0(\lambda t)\left(\int_0^{2R} J_0(\lambda t')g(z,t')dt'\right)\right.$$

$$\left. - J_0(\lambda t)\left(\int_0^{2R} N_0(\lambda t')g(z,t')dt'\right)\right]\lambda d\lambda.\qquad (13)$$

Here $J_0(t)$ and $N_0(t)$ are respectively the Bessel and Neumann functions of order 0, and $\mathbf{n}(z)$ is the vector of exterior normal to S. In $3D$, the formula looks simpler:

$$f(y) = -\frac{1}{8\pi^2}\mathrm{div}\int_S \mathbf{n}(z)\left(\frac{d}{dt}\frac{g(z,t)}{t}\right)\bigg|_{t=|z-y|} dA(z).\qquad (14)$$

This expression is equivalent to one of the formulas derived in [97] for the $3D$ case.

14

5.2   Series solutions for arbitrary geometries

Explicit inversion formulas for closed surfaces S different from spheres have not yet been found. There is, however, a different approach [59] that theoretically works for any closed S and that is practically useful when the surface is a boundary of a region whose eigenfunctions of the Dirichlet Laplacian are known.

Let λ_m^2 and $u_m(x)$ be the eigenvalues and normalized eigenfunctions of the Dirichlet Laplacian $-\Delta$ on the interior Ω of a closed surface S:

$$\Delta u_m(x) + \lambda_m^2 u_m(x) = 0, \qquad x \in \Omega, \quad \Omega \subseteq \mathbb{R}^n, \tag{15}$$
$$u_m(x) = 0, \qquad x \in S,$$
$$||u_m||_2^2 \equiv \int_\Omega |u_m(x)|^2 dx = 1.$$

As before, we would like to reconstruct a compactly supported function $f(x)$ from the known values of its spherical integrals $g(z, r)$ (8).

According to [59], $f(x)$ can be computed in the form of the Fourier series

$$f(x) = \sum_{m=0}^\infty \alpha_m u_m(x), \tag{16}$$

with the coefficients α_m computed by the formula

$$\alpha_m = \int_{\partial\Omega} I(z, \lambda_m) \frac{\partial}{\partial\mathbf{n}} u_m(z) dA(z) \tag{17}$$

where

$$I(z, \lambda_m) = \int_{\mathbb{R}^+} g(z, r) \Phi_{\lambda_m}(r) dr,$$

and $\Phi_{\lambda_m}(|x - z|)$ is a free-space rotationally invariant Green's function of the Helmholtz equation (15). Formula (17) is obtained by substituting the Helmholtz representation for $u_m(x)$

$$u_m(x) = \int_{\partial\Omega} \Phi_{\lambda_m}(|x - z|) \frac{\partial}{\partial\mathbf{n}} u_m(z) ds(\mathbf{z}) \qquad x \in \Omega, \tag{18}$$

into the expression for the projections $g(z, t)$.

15

Certainly, the need to know the spectrum and eigenfunctions of the Dirichlet Laplacian imposes a severe constraint on the surface S. However, there are simple cases, e.g. of a cube S, when such knowledge is readily available. As it was shown in [59], using the cubic surface S leads to a robust and fast reconstruction.

5.3 Examples of reconstructions and additional remarks about the inversion formulas

- All analytic (backprojection type) formulas (9)-(13) work equally well. See, for example the results of an analytic formula reconstruction in $3D$ shown in Fig. 5.
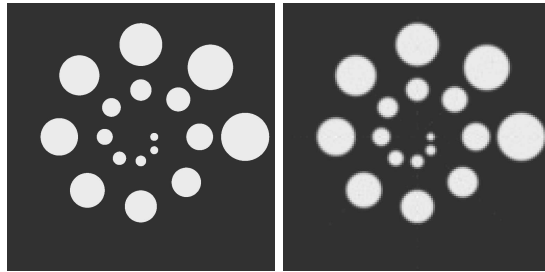

Figure 5: A mathematical phantom in $3D$ (left) and its reconstruction using an analytic inversion formula.

- It is worth noting that although formulas (9)-(10) and (12)-(14) will yield identical results when applied to functions that can be represented as the spherical mean Radon transform of a function supported inside S, they are in general not equivalent when applied to functions with larger supports. Simple examples (e.g., of f being the characteristic set of a large ball containing S) show that these two types of formulas provide different reconstructions.

- An interesting observation is that backprojection formulas (9)-(13) do not reconstruct the function f correctly inside the surface S, if f has support reaching outside S. For instance, applying the reconstruction formulas to the function $R_S(\chi_{|x|\leq 3})$ leads to an incorrect reconstruction of the value of $f = \chi_{|x|\leq 3}$ inside $S = \{|x| \leq 1\}$.

16

An another example: if one adds to the phantom shown in Fig. 5 two balls to the right of the surrounding sphere S, this leads to strong artifacts, as seen on Fig. 6.
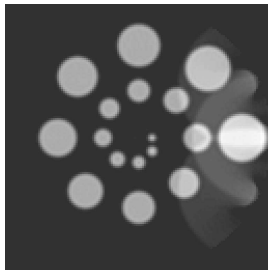

Figure 6: A perturbed reconstruction, due to presence of two additional balls outside S (not shown on the picture).

What is the reason for such a distortion? If one does not know in advance that f has support inside S, the backprojection formulas shown before use insufficient information to recover a function with a larger support, and thus uniqueness of reconstruction is lost. The formulas misinterpret the data, wrongly assuming that they came form a function supported inside S and thus reconstructing the function incorrectly.

Notice that the series reconstruction of the preceding Section is free of such problem. E.g., the reconstruction shown in Fig. 7 shows this.

6 Partial data. "Visible" and "invisible" singularities

Uniqueness of reconstruction does not imply practical recoverability, since the reconstruction procedure might be severely unstable. This is well known to be the case, for instance, in incomplete data situations in X-ray tomography, and even for complete data problems in electrical impedance tomography [52, 57, 65, 66].

A microlocal analysis done in [86], showed which parts of the wave front of a function f can be recovered from its partial X-ray data. An analog of this result also holds for the spherical mean transform R_S [62] (see also [100]
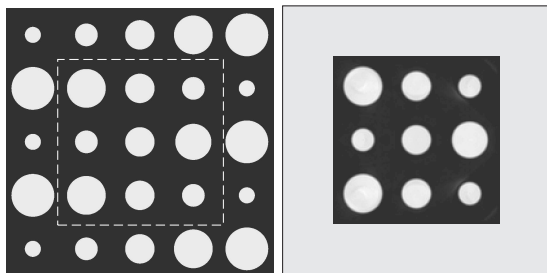
Figure 7: The phantom shown on the left includes several balls located outside the square acquisition surface S. This does not perturb the reconstruction inside S (right).

for a practical discussion). We formulate it below in an imprecise form (see [62] for precise formulation).

Theorem 6. *[62] A wavefront set point (x, ξ) of f is "stably recoverable" from $R_S f$ if and only if there is a circle (sphere in higher dimensions) centered on S, passing through x, and normal to ξ at this point.*

As we have already mentioned, this result does not exactly hold the way it is formulated and needs to include some precise conditions (see [62, Theorem 3]). The problem is that some cancellations of wave front points can occur. The statement is, for instance, correct if S is a smooth hypersurface and the support of f lies on one side of the tangent plane to S at the center of the sphere mentioned in the theorem.

Talking about jump singularities only (i.e., interfaces between smooth regions inside the object to be imaged), this result says that in order for a piece of the interface to be stably recoverable (dubbed "visible"), one should have for each point of this interface, a sphere centered at S and tangent to the interface at this point. Otherwise, the interface will be blurred away (even if there is a uniqueness of reconstruction theorem). The reason is that if all spheres of integration are transversal to the interface, the integration smoothes off the singularity, and its recovery becomes unstable. The Figure 8 below shows an example of an incomplete data reconstruction from spherical mean data. One sees clearly the effect of disappearence of the parts of the boundaries that are not touched tangentially by circles centered at transducers' locations.
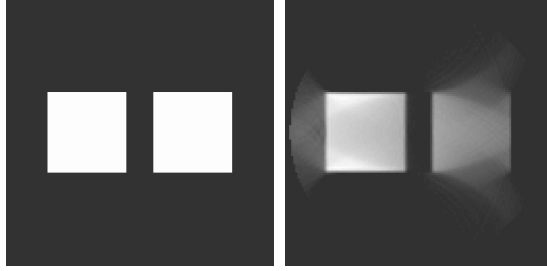
18

Figure 8: Effect of incomplete data: the phantom (left) and its incomplete data reconstruction. The transducers were located along a 180° circular arc (the left half of a large circle surrounding the squares).

7   Range conditions

The ranges of Radon type transforms are usually of infinite co-dimension in the appropriate function spaces. Knowing the range is useful for many theoretical and practical purposes (reconstruction algorithms, error corrections, incomplete data completion, etc.), and thus has attracted a lot of attention (e.g., [22, 28, 29, 30, 42, 43, 52, 55, 56, 57, 63, 65, 66, 72, 75, 81]).

For instance, for the standard Radon transform

$$f(x) \to g(s, \omega) = \int\limits_{x \cdot \omega = s} f(x) dx, |\omega| = 1,$$

the range conditions on $g(s, \omega)$ are:

1. *evenness*: $g(-s, -\omega) = g(s, \omega)$

2. *moment conditions*: for any integer $k \geq 0$, the kth moment

$$G_k(\omega) = \int\limits_{-\infty}^{\infty} s^k g(\omega, s) ds$$

   extends from the unit circle of vectors ω to a homogeneous polynomial of degree k in ω.

The evenness condition is obviously necessary and is kind of "trivial". It seems that the only non-trivial conditions are the moment ones. However,

19

here the standard Radon transform is misleading. In fact, for more general transforms of Radon type it is often easy (or easier) to find analogs of the moment conditions, while counterparts of the evenness conditions are often elusive (see [52, 55, 56, 65, 66, 72]). The same happens with the spherical mean transform R_S.

An analog of the moment conditions was already present implicitly (without saying that these were range conditions) in [5, 60, 61] and explicitly formulated as such in [16, 80]. Indeed, our discussion in Section 4 of the polynomials Q_k provides the following conditions of the moment type [5, 60, 61, 80]:

Moment conditions *on data* $g(p, r) = R_S f(p, r)$ *are: for any integer* $k \geq 0$, *the moment*

$$M_k(\omega) = \int_0^\infty r^{2k+d-1} g(p, r) dr$$

can be extended from S to a (non-homogeneous) polynomial $Q_k(x)$ of degree at most $2k$.

These conditions, however, are incomplete, and in fact infinitely many others, which play the role of an analog of eveness, need to be added.

Complete range descriptions for R_S when S is a sphere in $2D$ were discovered recently in [11] and then in odd dimensions in [25]. They were then extended to any dimension and interpreted in several different ways in [4]. These conditions happen to be intimately related to PDEs and spectral theory.

Let, as before, B be the unit ball in $\mathbb{R}^d$, $S = \partial B$ - the unit sphere, and C - the cylinder $B \times [0, 2]$ (see Fig. 9).
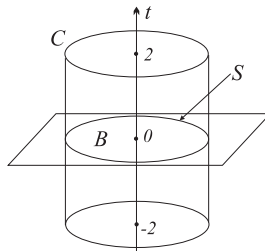

Figure 9: An illustration to the range description.

20

We introduce the spherical mean operator R_S as before:

$$R_S f(x,t) = G(x,t) = \int_{|y|=1} f(x+ty)dA(y).$$

Notice that if $G(x,t)$ is defined by the same formula for all $x \in \mathbb{R}^d$, then it satisfies Darboux equation [14, 19, 47]

$$G_{tt} + (d-1)t^{-1}G_t = \Delta_x G.$$

Moreover, inside the cylinder C, $G(x,t)$ vanishes when $t \geq 2$ (since the spheres of integration do not intersect the support of the function when $t \geq 2$).

The range description is now provided by the following results proven in [4]:

Theorem 7. *[4] The following four statements about a function $g \in C_0^\infty(S \times [0,2])$ are equivalent:*

1. *Function g is representable as $R_S f$ for some $f \in C_0^\infty(B)$.*

2. *(a) The moment conditions are satisfied.*

   (b) The solution $G(x,t)$ of the interior Darboux problem satisfies the condition

$$\lim_{t \to 0} \int_B \frac{\partial G}{\partial t}(x,t)\phi(x)dx = 0$$

   for any eigenfunction $\phi(x)$ of the Dirichlet Laplacian in B.

3. *(a) The moment conditions are satisfied.*

   (b) Let $-\lambda^2$ be an eigenvalue of Dirichlet Laplacian in B and ψ_λ the corresponding eigenfunction. Then the following orthogonality condition is satisfied:

$$\int_{S \times [0,2]} g(x,t)\partial_\nu \psi_\lambda(x)j_{n/2-1}(\lambda t)t^{n-1}dxdt = 0. \qquad (19)$$

   Here $j_p(z) = c_p \frac{J_p(z)}{z^p}$ is the so called spherical Bessel function.

4. *(a) The moment conditions are satisfied.*

21

(b) Let $\widehat{g}(x,\lambda) = \int g(x,t)j_{n/2-1}(\lambda t)t^{n-1}dt$. Then, for any $m \in \mathbb{Z}$, the mth spherical harmonic term $\widehat{g}_m(x,\lambda)$ of $\widehat{g}(x,\lambda)$ vanishes at non-zero zeros of Bessel function $J_{m+n/2-1}(\lambda)$.

Theorem 8. *[4]*

1. *In odd dimensions, moment conditions are not necessary, and thus conditions (b) alone suffice. (A similar earlier result was established for a related transform in [25].)*

2. *The range descriptions work in Sobolev scale $H_s \mapsto H_{s+(d-1)/2}$. (This uses a recent result by Palamodov [76]).*

3. *The range conditions 2 and 3 of the previous Theorem are necessary when S is the boundary of any bounded domain.*

8 Concluding remarks

8.1 Planar and linear transducers

Assuming that transducers are point-like, is clearly an approximation, and in fact, a transducer measures the average pressure over its area. It has been rightfully claimed that the point approximation for transducers should lead to some blurring in the reconstructions. This, as well as intricacies of reconstructions from the data obtained by point transducers, triggered recent proposals for different types of transducers (see [17, 18], [36]-[41], [77, 78]).

In these papers, it was suggested to use either planar, or line detectors.

In the first case [36], the detectors are assumed to be large and planar, ideally assumed to be approximations of infinite planes that are placed tangentially to a sphere containing the object. Thus, the data one collects is the integrals of the pressure over these planes, for all values of $t > 0$.

If one takes the standard $3D$ Radon transform of the pressure $p(x,t)$ with respect to x:

$$p(x,t) \mapsto q(s,t,\omega) = \int_{x\cdot\omega=s} p(x,t)dA(x),$$

where dA is the surface measure and ω is a unit vector in $\mathbb{R}^3$, this is well known to reduce the $3D$ Laplace operator Δ_x to the second derivative $\partial^2/\partial s^2$

22

[22, 28, 29, 30, 42, 43], and thus the $3D$ wave equation to the string vibration problem. The measured data provide the boundary conditions for this problem. The initial conditions in (1) mean evenness with respect to time, and thus the standard d'Alambert formula leads to the immediate realisation that the measured data is just the $3D$ Radon transform of $f(x)$. Hence, the reconstruction boils down to the well known inversion formulas for the Radon transform.

Another proposal ([17, 18], [38]-[41], [77, 78]) is to use line detectors that provide line integrals of the pressure $p(x, t)$. Such detectors can be implemented optically, using either Fabry-Perot [17], or Mach-Zehnder [78] interferometers.

Suppose that the object is surrounded by a surface that is rotation invariant with respect to the z-axis. It is suggested to place the line detectors perpendicular to the z-axis and tangential to the surface. The same consideration as above then shows that after applying the $2D$ Radon (or X-ray, which in $2D$ is the same) transform in each plane orthogonal to z-axis, the $3D$ wave equation converts into the $2D$ one for the Radon data. The measurements provide the boundary data. Thus, the reconstruction boils down to solving a $2D$ problem similar to the one in the case of point detectors, and then inverting the $2D$ Radon transform.

Due to the recent nature of these two projects, it appears to be too early to judge which one will be superior in the end. For instance, it is not clear beforehand, whether the approximation of infinite size (length, area) of the linear or planar detectors works better than the zero dimension approximation for point detectors. Further studies should resolve these questions.

8.2   Uniqueness

Albeit, as it was mentioned, one can consider the practical problems about uniqueness resolved, the mathematical understanding of the uniqueness problem for the restricted spherical mean operators R_S is still unsatisfactory. Here are some questions that still await their resolution:

1. Describe uniqueness sets in dimensions larger than 2 (prove the Conjecture 4). Recent limited progress, as well as variations on this theme can be found in [1]-[10].

2. Prove Theorem 3 without using microlocal and harmonic polynomial tools.

3. Prove an analog of Theorem 3 for the hyperbolic plane.

4. Prove Theorem 3 on uniqueness sets S under the condition of sufficiently fast decay (rather than compactness of support) of the function. Very little is known for the case of functions without compact support. The main known result is of [3], which decribes for which values of $1 \leq p \leq \infty$ the result of Corollary 2 still holds:

   Theorem 9. *[3] Let S be the boundary of a bounded domain in $\mathbb{R}^d$ and $f \in L^p(\mathbb{R}^d)$ such that $R_S f \equiv 0$. If $p \leq 2d/(d-1)$, then $f \equiv 0$ (and thus S is injectivity set for this space). This fails for any $p > 2d/(d-1)$.*

   An analog of this theorem is also proven for Riemannian symmetric spaces of rank 1.

8.3   Inversion

Albeit closed form (backprojection type) inversion formulas are available now for the cases of S being a plane (and object on one side from it), cylinder, and a sphere, there is still a lot of mistery surrounding this issue.

1. It would be interesting to understand whether (closed form, rather than series expansion) inversion formulas could be written for non-spherical acquisition surfaces S.

2. The I. Gelfand's school of integral geometry has developed a marvelous machinery of the so called κ operator, which provides a general approach to inversion and range descriptions for transforms of Radon type [28, 29]. In particular, it has been applied to the case of integration over various collections ("complexes") of spheres in [29, 31]. This consideration seem to suggest that one should not expect explicit closed form inversion formulas for R_S when S is a sphere. We, however, know that such formulas have been discovered recently [26, 58]. This apparent controversy has not been resolved.

8.4   Stability

Stability of inversion when S is a sphere surrounding the support of $f(x)$ is the same as for the standard Radon transform, as the results of [76] and second statement of Theorem 8 show. However, if the support reaches outside,

albeit Corollary 2 still guarantees uniqueness of reconstruction, stability (at least for the parts outside S) is gone. Indeed, Theorem 6 shows that some parts of singularities of f outside S will not be stably "visible."

8.5   Range

As Theorem 6 states, the range conditions 2 and 3 of Theorem 7 are necessary also for non-spherical closed surfaces S and for functions with support outside S. They, however, are not expected to be sufficient, since Theorem 6 indicates that one might expect non-closed ranges in some cases.

8.6   Miscellaneous

1. We have made a serious assumption of the sound speed being constant. Although it seems to work fine, for instance, in mammography (at least on the earliest stages of cancer), it is clearly incorrect even in this case. The study of the influence of variability of the wave speed on different facets of TAT is just in the beginning stage (e.g., [53, 46]).

2. The TAT model we have considered can be called "active thermoacoustic tomography," due to the set-up when the practitioner creates the signal. There has been some recent development of the "passive thermoacoustic tomography," where the thermoacoustic signal is used to image the themperature sources present inside the body. One can find a survey of this area in [79].

Acknowledgments

References

[1] M. L. Agranovsky, Radon transform on polynomial level sets and related problems, Israel Math. Conf. Proc., **11** (1997), 1–21.

[2] M. Agranovsky, On a problem of injectivity for the Radon transform on a paraboloid, in Analysis, geometry, number theory: the mathematics of Leon Ehrenpreis (Philadelphia, PA, 1998), Contemp.Math. v. 251, AMS, Provodence, RI, 2000, 1–14.

[3] M. Agranovsky, C. Berenstein, and P. Kuchment, Approximation by spherical waves in L^p-spaces, J. Geom. Anal. **6** (1996), no. 3, 365–383.

[4] M. Agranovsky, P. Kuchment, and E. T. Quinto, Range descriptions for the spherical mean Radon transform, arXiv:math.AP/0606314, to appear in J. Funct. Anal.

[5] M. Agranovsky and E.T. Quinto, Injectivity sets for the Radon transform over circles and complete systems of radial functions, J. Funct. Anal. **139** (1996), 383-414.

[6] M. L. Agranovsky, E. T. Quinto, Geometry of stationary sets for the wave equation in $\mathbb{R}^n$:the case of finitely suported initial data, Duke Math.J., **107** (2001), no. 1, 57–84.

[7] M. L. Agranovsky, E. T. Quinto, Stationary sets for the wave equation in crystallographic domains, Trans. AMS, **355** (2003), no. 6, 2439–2451.

[8] M. L. Agranovsky, E. T. Quinto, Remarks on stationary sets for the wave equation, Integral Geometry and Tomography, Contemp. Math., v. 405, 2006, 1–11.

[9] M. L. Agranovsky, V. V. Volchkov, L. Zalcman, Conical uniqueness sets for the spherical Radon transform, Bull. London Math. Sos. **31** (1999), no. 4, 363–372.

[10] G. Ambartsoumian and P. Kuchment, On the injectivity of the circular Radon transform, Inverse Problems 21 (2005), 473-485.

[11] G. Ambartsoumian and P. Kuchment, A range description for the planar circular Radon transform, SIAM J. Math. Anal. vol. 38, no. 2, 2006, 681-692.

[12] G. Ambartsoumian and S. Patch, Thermoacoustic tomography - implementation of exact backprojection formulas, arXiv:math.NA/0510638.

[13] L.-E. Andersson, On the determination of a function from spherical averages, SIAM J. Math. Anal. **19** (1988), no. 1, 214–232.

[14] L. Asgeirsson, Über eine Mittelwerteigenschaft von Lösungen homogener linearer partieller Differentialgleichungen zweiter Ordnung mit konstanten Koeffizienten, Ann. Math., **113** (1937), 321–346.

[15] G. Beylkin, The inversion problem and applications of the generalized Radon transform, Comm. Pure Appl. Math. 37(1984), 579–599.

[16] E. Bouzaglo-Burov, Inversion of spherical Radon transform, methods and numerical experiments, MS Thesis, Bar-Ilan Univ., 2005, 1–30. (In Hebrew)

[17] P. Burgholzer, C. Hofer, G. Paltauf, M. Haltmeier, and O. Scherzer, Thermoacoustic tomography with integrating area and line detectors. IEEE Transactions on Ultrasonics, Ferroelectrics, and Frequency Control **52(9)** (2005), 1577–1583.

[18] P. Burgholzer, C. Hofer, G. J. Matt, G. Paltauf, M. Haltmeier, and O. Scherzer, Thermoacoustic tomography using a fiber-based Fabry-Perot interferometer as an integrating line detector, Proc. SPIE **6086** (2006), 434–442.

[19] R. Courant and D. Hilbert, *Methods of Mathematical Physics, Volume II Partial Differential Equations*, Interscience, New York, 1962.

[20] A. Denisjuk, Integral geometry on the family of semi-spheres. Fract. Calc. Appl. Anal. **2**(1999), no. 1, 31–46.

[21] G. J. Diebold, T. Sun, M. I. Khan, Photoacoustic monopole radiation in one, two, and three dimensions, Phys. Rev. Lett. **67** (1991), no. 24, 3384–3387.

[22] L. Ehrenpreis, *The Universality of the Radon Transform*, Oxford Univ. Press 2003.

[23] J. A. Fawcett, Inversion of n-dimensional spherical averages, SIAM J. Appl. Math. **45**(1985), no. 2, 336–341.

[24] D. Finch, M. Haltmeier, and Rakesh, Inversion of spherical means and the wave equation in even dimensions, preprint arXiv math.AP/0701426.

[25] D. Finch and Rakesh, The range of the spherical mean value operator for functions supported in a ball, Inverse Problems **22** (2006), 923-938.

[26] D. Finch, S. Patch, and Rakesh, Determining a function from its mean values over a family of spheres, SIAM J. Math. Anal. **35** (2004), no. 5, 1213–1240.

[27] L. Flatto, D. J. Newman, H. S. Shapiro, The level curves of harmonic functions, Trans. Amer. Math. Soc. **123** (1966), 425–436.

[28] I. Gelfand, S. Gindikin, and M. Graev, Integral geometry in affine and projective spaces, J. Sov. Math. 18(1980), 39–167.

[29] I. Gelfand, S. Gindikin, and M. Graev, *Selected Topics in Integral Geometry*, Transl. Math. Monogr. v. 220, Amer. Math. Soc., Providence RI, 2003.

[30] I. Gelfand, M. Graev, and N. Vilenkin, *Generalized Functions, v. 5: Integral Geometry and Representation Theory*, Acad. Press 1965.

[31] S. Gindikin, Integral geometry on real quadrics, in *Lie groups and Lie algebras: E. B. Dynkin's Seminar*, 23–31, Amer. Math. Soc. Transl. Ser. 2, 169, Amer. Math. Soc., Providence, RI, 1995.

[32] A. Greenleaf and G. Uhlmann, Microlocal techniques in integral geometry, Contemporary Math. **113** (1990), 149–155.

[33] V. Guillemin, Fourier integral operators from the Radon transform point of view, Proc. Symp. Pure Math., 27 (1975) 297–300.

[34] V. Guillemin, On some results of Gelfand in integral geometry, Proc. Symp. Pure Math., 43(1985) 149–155.

[35] V. Guillemin and S. Sternberg *Geometric Asymptotics*, Amer. Math. Soc., Providence, RI, 1977.

[36] M. Haltmeier, P. Burgholzer, G. Paltauf and O. Scherzer, Thermoacoustic computed tomography with large planar receivers, Inverse Problems **20** (2004), 1663–1673.

[37] M. Haltmeier, T. Schuster, and O. Scherzer, Filtered backprojection for thermoacoustic computed tomography in spherical geometry, Mathematical Methods in the Applied Sciences, **28** (2005), 1919–1937.

[38] M. Haltmeier, G. Paltauf, P. Burgholzer, and O. Scherzer, Thermoacoustic Tomography with integrating line detectors, Proc. SPIE 5864:586402-8. 2005.

[39] M. Haltmeier, P. Burgholzer, C. Hofer, G. Paltauf, R. Nuster and O. Scherzer, Thermoacoustic tomography using integrating line detectors, Ultrasonics Symposium **1** (2005), 166–169.

[40] M. Haltmeier, O. Scherzer, P. Burgholzer, and G. Paltauf, Thermoacoustic Computed Tomography with large planar receivers, ECMI Newsletter 37, pp. 31-34, 2005. http://www.it.lut.fi/mat/EcmiNL/ecmi37/

[41] M. Haltmeier, T. Fidler, Mathematical Challenges Arising in Thermoacoustic Tomography with Line Detectors, preprint arXiv:math.AP/0610155.

[42] S. Helgason, *The Radon Transform*, Birkhäuser, Basel 1980.

[43] S. Helgason, *Groups and Geometric Analysis*, Amer. Math. Soc., Providence, R.I. 2000.

[44] G. Herman (Ed.), *Image Reconstruction from Projections* , Topics in Applied Physics, v. 32, Springer Verlag, Berlin, New York 1979.

[45] L. Hörmander, *The Analysis of Linear Partial Differential Operators*, vol. 1, Springer-Verlag, New York 1983.

[46] X. Jin, and L. V. Wang, Thermoacoustic tomography with correction for acoustic speed variations, Physics in Medicine and Biology **51** (2006), 6437?-6448.

[47] F. John, *Plane Waves and Spherical Means, Applied to Partial Differential Equations*, Dover 1971.

[48] A. C. Kak, M. Slaney, *Principles of Computerized Tomographic Imaging*, SIAM, Philadelphia 2001.

[49] R. A. Kruger, W. L. Kiser, D. R. Reinecke, and G. A. Kruger, Thermoacoustic computed tomography using a conventional linear transducer array, Med. Phys. **30 (5)** (2003), 856–860.

[50] R. A. Kruger, P. Liu, Y. R. Fang, and C. R. Appledorn, Photoacoustic ultrasound (PAUS)reconstruction tomography, Med. Phys. **22** (1995), 1605-1609.

[51] P. Kuchment, unpublished, 1993.

[52] P. Kuchment, Generalized Transforms of Radon Type and Their Applications, in [73], pp. 67–91.

[53] P. Kuchment, On injectivity problem in thermoacoustic tomography, in preparation.

[54] P. Kuchment, K. Lancaster, and L. Mogilevskaya, On local tomography, Inverse Problems, 11(1995), 571–589.

[55] P. Kuchment and S. Lvin, Paley-Wiener theorem for the exponential Radon transform, Acta Applicandae Mathematicae, no.18, 1990, 251–260.

[56] P. Kuchment and S. Lvin, The Range of the Exponential Radon Transform, Soviet Math Dokl, **42** (1991) , no.1, 183–184.

[57] P. Kuchment and E. T. Quinto, Some problems of integral geometry arising in tomography, chapter XI in [22].

[58] L. Kunyansky, Explicit inversion formulae for the spherical mean Radon transform, Inverse Problems **23** (2007), pp. 373–383.

[59] L. Kunyansky, A series solution and a fast algorithm for the inversion of the spherical mean Radon transform, preprint arXiv math.AP/0701236.

[60] V. Lin and A. Pinkus, Fundamentality of ridge functions, J. Approx. Theory, 75(1993), 295-311.

[61] V. Lin and A. Pinkus, Approximation of multivariate functions, in Advances in computational mathematics, H. P. Dikshit and C. A. Micchelli, Eds., World Sci. Publ., 1994, 1-9.

[62] A. K. Louis and E. T. Quinto, Local tomographic methods in Sonar, in *Surveys on solution methods for inverse problems*, pp. 147-154, Springer, Vienna, 2000.

[63] S. Lvin, Data correction and restoration in emission tomography, pp. 149–155 in E.T. Quinto, M. Cheney, and P. Kuchment (Editors), *Tomography, Impedance Imaging, and Integral Geometry*, Lectures in Appl. Math., vol. 30, AMS, Providence, RI 1994.

[64] *Mathematics and Physics of Emerging Biomedical Imaging*, The National Academies Press 1996. Available online at http://www.nap.edu/catalog.php?record_id=5066#toc.

[65] F. Natterer, *The mathematics of computerized tomography*, Wiley, New York, 1986.

[66] F. Natterer and F. Wübbeling, *Mathematical Methods in Image Reconstruction*, Monographs on Mathematical Modeling and Computation v. 5, SIAM, Philadelphia, PA 2001.

[67] M. M. Nessibi, L. T. Rachdi, K. Trimeche, Ranges and inversion formulas for spherical mean operator and its dual, J. Math. Anal. Appl. 196 (1995), no. 3, 861–884.

[68] S. Nilsson, Application of fast backprojection techniques for some inverse problems of integral geometry, Linkoeping studies in science and technology, Dissertation 499, Dept. of Mathematics, Linkoeping university, Linkoeping, Sweden 1997.

[69] C. J. Nolan and M. Cheney, Synthetic aperture inversion, Inverse Problems **18**(2002), 221–235.

[70] S. J. Norton, Reconstruction of a two-dimensional reflecting medium over a circular domain: exact solution, J. Acoust. Soc. Am. **67** (1980), 1266-1273.

[71] S. J. Norton and M. Linzer, Ultrasonic reflectivity imaging in three dimensions: exact inverse scattering solutions for plane, cylindrical, and spherical apertures, IEEE Transactions on Biomedical Engineering, **28** (1981), 200–202.

[72] R. Novikov, On the range characterization for the two-dimensional attenuated X-ray transform, Inverse Problems **18** (2002), 677–700.

[73] G. Olafsson and E. T. Quinto (Editors), *The Radon Transform, Inverse Problems, and Tomography. American Mathematical Society Short Course January 3–4, 2005, Atlanta, Georgia*, Proc. Symp. Appl. Math., v. 63, AMS, RI 2006.

[74] V. P. Palamodov, Reconstruction from limited data of arc means, J. Fourier Anal. Appl. **6** (2000), no. 1, 25–42.

[75] V. P. Palamodov, *Reconstructive Integral Geometry*, Birkhäuser, Basel 2004.

[76] V. Palamodov, Remarks on the general Funk-Radon transform and thermoacoustic tomography, preprint arXiv:math/0701204.

[77] G. Paltauf, P. Burgholzer, M. Haltmeier, and O. Scherzer, Thermoacoustic Tomography using optical Line detection, Proc. SPIE **5864** (2005), 7–14.

[78] G. Paltauf, R. Nuster, M. Haltmeier, and P. Burgholzer, Thermoacoustic Computed Tomography using a Mach-Zehnder interferometer as acoustic line detector. Submitted

[79] V. I. Passechnik, A. A. Anosov, K. M. Bograchev, Fundamentals and prospects of passive thermoacoustic tomography, Critical reviews in Biomed. Eng. **28** (2000), no. 3&4, 603–640.

[80] S. K. Patch, Thermoacoustic tomography - consistency conditions and the partial scan problem, Phys. Med. Biol. **49** (2004), 1–11.

[81] I. Ponomarev, Correction of emission tomography data. Effects of detector displacement and non-constant sensitivity, Inverse Problems, **10** (1995) 1–8.

[82] D. A. Popov and D. V. Sushko, A parametrix for the problem of optical-acoustic tomography, Dokl. Math. **65** (2002), no. 1, 19–21.

[83] D. A. Popov and D. V. Sushko, Image restoration in optical-acoustic tomography, problems of Information Transmission **40** (2004), no. 3, 254–278.

[84] E. T. Quinto, The dependence of the generalized Radon transform on defining measures, Trans. Amer. Math. Soc. **257** (1980), 331–346.

[85] E. T. Quinto, Pompeiu transforms on geodesic spheres in real analytic manifolds, Israel J. Math. **84** (1993), 353–363.

[86] E. T. Quinto, Singularities of the X-ray transform and limited data tomography in $\mathbb{R}^2$ and $\mathbb{R}^3$, SIAM J. Math. Anal. **24** (1993), 1215–1225.

[87] E. T. Quinto, Radon transforms on curves in the plane, in *Tomography, Impedance Imaging,. and Integral Geometry*, 231–244, Lectures in Appl. Math., Vol. 30, Amer. Math. Soc. 1994.

[88] E. T. Quinto, An introduction to X-ray tomography and Radon transforms, in [73], pp. 1–23.

[89] A. G. Ramm, Inversion of the backscattering data and a problem of integral geometry. Phys. Lett. A **113** (1985), no. 4, 172–176.

[90] A. G. Ramm, Injectivity of the spherical means operator, C. R. Math. Acad. Sci. Paris **335** (2002), no. 12, 1033–1038.

[91] V. G. Romanov, Reconstructing functions from integrals over a family of curves, Sib. Mat. Zh. **7** (1967), 1206–1208.

[92] T. Schuster and E. T. Quinto, On a regularization scheme for linear operators in distribution spaces with an application to the spherical Radon transform, SIAM J. Appl. Math. **65 (4)** (2005), 1369–1387.

[93] P. Stefanov and G. Uhlmann, Integral geometry of tensor fields on a class of non-simple Riemannian manifolds, preprint arXiv:math/0601178.

[94] A. C. Tam, Applications of photoacoustic sensing techniques, Rev. Mod. Phys. **58** (1986), no. 2, 381–431.

[95] X. Wang, Y. Pang, G. Ku, X. Xie, G. Stoica, L. Wang, Noninvasive laser-induced photoacoustic tomography for structural and functional *in vivo* imaging of the brain, Nature Biotechnology, **21** (2003), no. 7, 803–806.

[96] M. Xu and L.-H. V. Wang, Time-domain reconstruction for thermoacoustic tomography in a spherical geometry, IEEE Trans. Med. Imag. **21** (2002), 814-822.

[97] M. Xu and L.-H. V. Wang, Universal back-projection algorithm for photoacoustic computed tomography, Phys. Rev. E **71** (2005), 016706.

[98] Y. Xu, D. Feng, and L.-H. V. Wang, Exact frequency-domain reconstruction for thermoacoustic tomography: I. Planar geometry, IEEE Trans. Med. Imag. **21** (2002), 823-828.

[99] Y. Xu, M. Xu, and L.-H. V. Wang, Exact frequency-domain reconstruction for thermoacoustic tomography: II. Cylindrical geometry, IEEE Trans. Med. Imag. **21** (2002), 829-833.

[100] Y. Xu, L. Wang, G. Ambartsoumian, and P. Kuchment, Reconstructions in limited view thermoacoustic tomography, Medical Physics 31(4) April 2004, 724-733.

[101] N. Zobin, unpublished, 1993.